Egypt.J.Chem. **Vol. 63**, No. 5. pp. 1955 - 1964 (2020)

Egyptian Journal of Chemistry
http://ejchem.journals.ekb.eg/

Preparation and Characterization of Phosphate Glasses Co-doped with Rare Earth Ions

A. A. Elbakey[1]*, M. A. Farag[2], M. El-Okr[3], T. Y. Elrasasi[1], M. K. El-Mansy[1]
[1]Physics Department, Faculty of Science, Benha University, Egypt.
[2]Physics Department, Faculty of Science, Al-Azhar University, Cairo, Egypt.
[3]Physics Department, Faculty of Science, Al-Azhar University, Cairo, Egypt. Deceased at Dec/2018.

SAMARIUM zinc sodium phosphate glasses doped by different Er_2O_3 concentrations were prepared using a conventional melt quenching technique. The structural properties due to the influence of Er^{+3} ions on the presented glass network were investigated. XRD pattern confirms samples amorphousity. Surface morphology using SEM proved the non-crystallinity and the homogeneity of the samples. The elemental composition using EDAX analysis gave an acceptable mass percentage of the constituent's elements. FTIR revealed the formation of Non-Bridging oxygen (NBO). The measured density, molar volume, ion concentration, interatomic distance, polaron radius and field strength have been studied with respect to the concentration of Er^{+3}.

Keywords: Rare earth element, Phosphate glass, Structural properties.

Introduction

The effect of rare-earth ions RE on glass network becomes one of the hot topics in glass science. Recently, glasses doped with (RE) oxides have received enormous attention due to their peculiar properties in different technological applications such as optical communication field [1], solid-state lasers such as mid-IR fiber laser [2] and frequency converters [3] . Great efforts have been done to search for host materials that are suitable for RE.

Glasses play a significant role for device applications cause they exhibit special advantages as the isotropy of its physical properties and the low cost of preparation [4]. The most interesting advantages of using the glasses as host materials are the possibility to shape through a simple and highly productive manufacturing process [5].

Glasses doped with rare-earth elements are known by their excellent chemical and physical properties like the higher chemical durability, inflater hardness, and elastic modulus due to the exaggerating field strength of these glasses than other traditional modifier cations [6]. Among the glass matrices, phosphate glasses present distinct optical properties such as large infrared transmission window, low melting point, and high gain intensity. The high gain intensity in phosphate glass is due to the unique nature of high solubility of activator ions doped into a relatively small volume [7]. However, the disadvantage of phosphate glasses is the weakness of chemical durability which has been overcome by the injection of alkali and alkaline earth metal oxides [8]. In general, RE cations are used mainly as a modifier for glasses network such that they combine with the space between PO_4 tetrahedral because Lanthanide's ionic radius decreases with the increasing of their atomic number, also, their field strength changes continuously with the change of the ionic radius [9]. This variation causes many various physical properties [10]. The tetrahedral phosphate PO_4 connected in the vitreous P_2O_5 by three corners of oxygens and the fourth one is doubly bonded [11]. The incorporation of any RE ion (modifier) in phosphate glasses results in the breaking down of the bridging bond of P–O–P bonds and the formation of a non- bridging bond of P–O–RE bonds [12]. According to the number of the bridging oxygen the structure of

*Corresponding author e-mail: ayaadel185@yahoo.com
Received 3/8/2019; Accepted 7/10/2019
DOI: 10.21608/ejchem.2019.15556.1944

the tetrahedral PO_4 could be described by a code Q^n used by Lippma et al. [13] where (n=[0,1,2,3] and represents the number of bridging oxygen). The Q^3 site denotes a fully polymerized neutral unit of structure, Q^2 is a structure based on chains and rings and it has a negative charge, Q^1 means two corner-sharing tetrahedral units and Q^0 means isolated tetrahedral [14]. Vibrational spectroscopy such as FTIR has been utilized to investigate the structural properties and identify the fundamental structural units which are very prerequisites for understanding the complex multicomponent systems [20,21].

Among the Lanthanides phosphate glasses, Er^{3+} doped glasses are especially attractive for numerous applications such as microchip lasers, erbium-doped fiber amplifiers (EDFA) in wavelength division multiplexing (WDM) systems, near-infrared telecommunication windows, and eye-safe laser systems [15]. Doping with Er^{+3} singly in glasses produces small absorption and emission cross-sections. While the codoping with other RE produces energy transfer between their levels and causes the needed enhancement [16]. Many research has been done on studying glasses doped with pairs of RE especially with Er^{+3} ion e.g. Yb^{+3}/Er^{+310}, Pr^{+3}/Er^{+3} [18] and Sm^{+3}/Er^{+3} [19].

In this paper, the influence of Er^{3+} ions on the structural properties of samarium zinc sodium phosphate glasses has been reported by employing various characterization techniques such as FTIR, XRD, SEM, EDX, and Density.

Experimental work

High purity of $(NH_4)_2HPO_4$, Li_2CO_3, ZnO, Na_2CO_3, Sm_2O_3 and Er_2O_3 were used to prepare a series of phosphate glasses in the chemical formula $40P_2O_5$-20ZnO-$10Li_2O$-Sm_2O_3-(29-x) Na2O-xEr_2O_3 as tabulated in Table 1, where x = 0, 1, 2, 3 Mol %. The starting materials accurately weighed and the batches were mixed and grinded well in an agate mortar. In order to remove bubbles, undesired gases and obtain homogeneous optical glass, a semi-continuous melting process is adopted. The batches were melted in a porcelain crucible at 1100 °C for one hour. The melt was cast onto a preheated brass mould at 300 °C to prevent the fast cooling. To reduce the internal strain, the glasses were annealed at 200 °C for 4h and then left the furnace to cool down to room temperature. X-ray diffraction (XRD) patterns were carried out using the Philips X'Pert system, working at Cu K_α radiation (λ = 1.54056 Å). Surface morphology and elemental composition of glasses were studied using a scanning electron microscope (SEM) accompanying Electron Dispersive X-ray spectroscopy (EDAX) (quanta-FEG250). Fourier Transform Infrared (FTIR) spectrometer, Perkin Elmer spectrometer, RTX, was used to study the local structure of the prepared glasses. The density of the samples was measured by the Archimedes principle using Toluene as an immersing liquid.

Results and Discussion

X-Ray Diffraction (XRD)

XRD spectra of the prepared samples are shown in Fig. 1. The absence of sharp peaks in XRD patterns indicates the non-crystallinity of the prepared samples [18,19] *SEM & EDX*

The SEM analysis indicates the nature of homogeneity, moreover, the absence of any feature or particle formation assuring the amorphousity state of the presented glass samples. As shown in Fig. 2 (a, b) for Sm_0Er_0 and Sm_1Er_0 respectively. The elemental composition results of EDAX are in good agreement with the calculated mass percentage of the batch's composition especially the presence of Sm^{+3} ions by (nearly 1 mol%) as presented in Fig. 2 (c, d) for Sm_0Er_0 and Sm_1Er_0 respectively [24].

FTIR analysis

Fig. 3 shows the FTIR spectra in the range between 1400 and 400 cm^{-1} of all prepared samples. The row data were deconvoluted using eight independent Gaussian components shown in Fig. 4.(a,b,c,d,e). The bands in the range of 460 – 418 cm^{-1} were assigned as the bending vibrations of O-P-O units, δ (PO_4) modes of (PO_2) in chain groups [25]. The bands about 552-568 cm^{-1} were assigned to O-P=O bending vibration [26]. The absorption bands υ_{as}(P–O–P) and υ_s(P–O–P) occurring around 889-905 cm^{-1} and 736-749 cm^{-1} are assigned to the asymmetric and symmetric stretching of the bridging oxygen atoms bonded to a phosphorus atom in a Q^2 phosphate tetrahedron respectively [27]. The bands near 977-988 cm^{-1} were assigned to the symmetric stretching vibration of $P\text{-}O^-$ mode in the Q^1, while the strong IR band located about 1100 cm^{-1} was related to the asymmetric stretching vibration of the $P\text{-}O^-$ mode in the Q^2 units [28]. The Peaks in spectral range 1174-1196 cm^{-1} occurred due to PO_2 symmetrical stretching although bands near 1282-1264 cm^{-1}

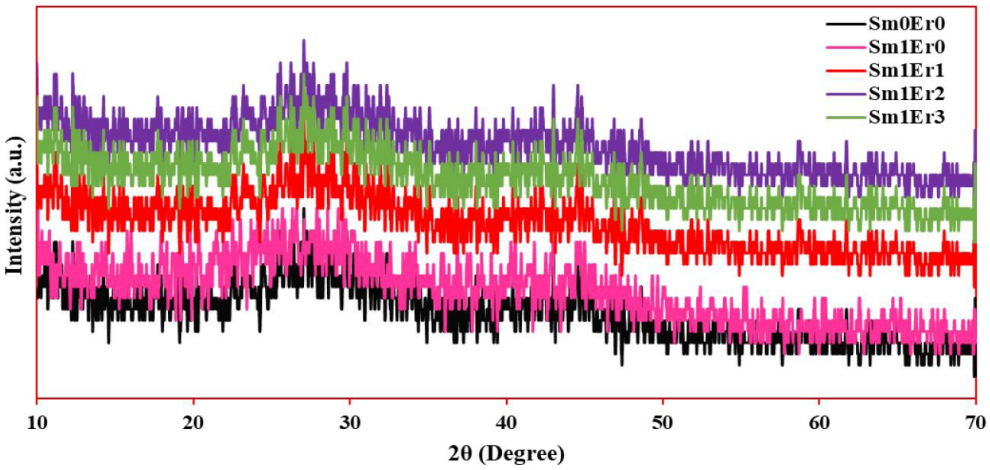

Fig.1: XRD patterns of the prepared samples at different concentrations of Er^{+3}.

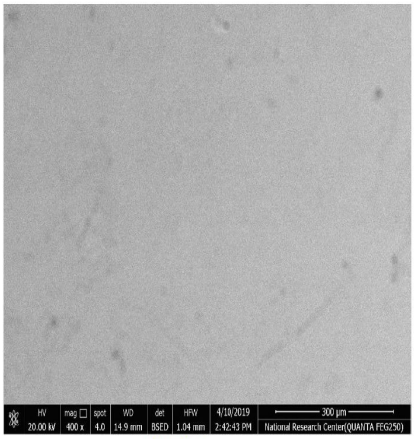

Fig.2(a)

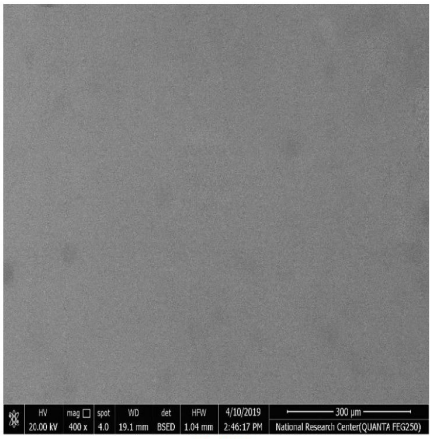

Fig.2(b)

Fig.2: (a,b) SEM for Sm0Er0 and Sm1Er0 respectively.

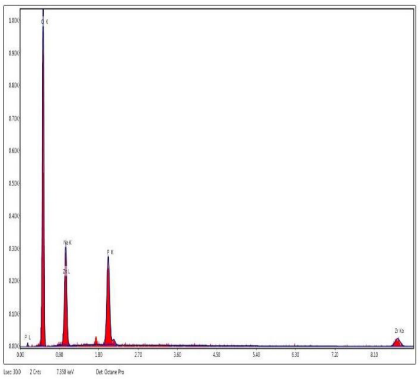

Fig.2(c)

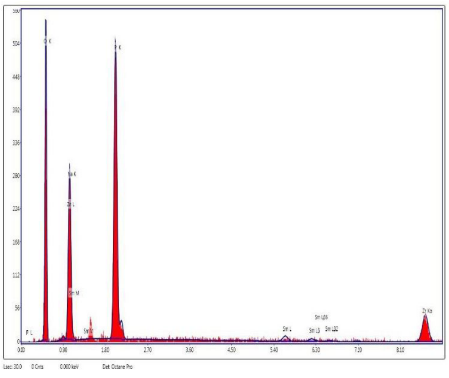

Fig.2(d)

Fig.2 : (c,d) EDX for for Sm0Er0 and Sm1Er0 respectively.

may be attributed to asymmetric stretching mode of the two non-bridging oxygen atoms bonded to phosphorus atoms, the O–P–O or (PO_2) υ_{as} units, in the phosphate tetrahedral and the stretching mode of P=O double bonds. These two bands, (PO_2) as and P=O, are overlapped to form broader bands in the spectra [29]. The main assignment of FTIR spectra for the deconvoluted bands for the studied glass samples is listed in Table 2.

The injection of Er^{+3} and Sm^{+3} ions into the phosphate glass caused a serious change in the metaphosphate glass which observed by the changes occurred in the intensities and the positions of peaks. It clearly appeared from Fig. 3 that all positions of the IR peaks slightly shifted towards the higher frequency, This shifting is attributed to the decreasing in the bond length confirming the formation of NBO in the system as reported in[30]. It is observed that the intensity of the bridging bond (P-O-P) which is centered at (737-746) cm^{-1} decreased quietly by the introducing of the modifiers Sm^{+3} and Er^{+3} ions. The addition of rare earth elements caused a breaking down of the polymerized chains of the phosphate glass to depolymerizing phase forming more NBO[31]. In the presented system, the doping of Sm^{+3} and Er^{+3} ions are at the expense of Na_2O ions, and it is known that the addition of alkali oxide i.e (Na_2O) easily caused breaking in the bridging bond and forming NBO[25]. The decreasing of (Na_2O) with (30-26)% mole concentration in the presence of increasing rare-earth ions caused no more long-chain existed in the glassy system confirming the huge amount of non-bridging bonds [13]. So the non-bridging bond (P=O) which is peaked around (1252-1277) cm^{-1} increased slowly and seemed to had almost a constant intensity by the influencing of Sm^{+3} and Er^{+3} ions.

Density and Molar volume

Fig. 5 shows the variation of density and molar volume with the influence of Er_2O_3 ions. Firstly, it is observed that the density of the blank sample (Sm_0Er_0) which is free from modifiers increased by 12% and decreased by 8% in the molar volume due to the singly doping of Sm_2O_3. By the introducing of erbium oxide, the density increases slightly in a gradual manner. This behavior attributed to the doping of higher molecular weight of Sm^{+3} and Er^{+3} than Na^{-} [32], on the other hand, the molar volume (V_m) has two different regions in the same respect. The first region represents decreasing in the molar volume which indicates that the ionic radius of the modifiers are smaller than the interstices of the system network [16], while the enlarge in molar volume above 1 mol % of Er_2O_3 is due to the formation of non-bridging oxygens (NBOs) and opens up the structure of the prepared glass network [33]. The open structure may be also due to the inability of the voids of the phosphate network to accommodate such modifier ions without any expansion of the glass matrix [34].

The average distance between phosphorous ions, d_{p-p} and V_m^p the molar volume that contains one mole of phosphorous were determined using equations (1, 2) [24].

$$d_{p-p} = \left(\frac{V_m^p}{N_A}\right)^{1/3} \quad (1)$$

$$V_m^p = \frac{V_m}{2(1-X_n)} \quad (2)$$

where, is the Avogadro's number and is the mole fraction of P_2O_5.

The ionic concentration N_i, interatomic distance r_i, and polaron radius r_p and the field strength F have been calculated as a function of Er^{+3} according to the following equations [29-30-37].

$$N_i = \frac{C_i N_A}{M_w} X \rho \quad (3)$$

$$r_i = \left[\frac{1}{N_i}\right]^{1/3} \quad (4)$$

$$r_p = \frac{1}{2}\left(\frac{\pi}{6 N_i}\right)^{1/3} \quad (5)$$

$$F = \frac{z}{(r_i)^2} \quad (6)$$

where is the sample's density, C_i, Mw and z are the mole concentration %, molecular weight and the oxidation number of Er^{+3} ions respectively. From Fig. 6 It is observed that the follows the same trend as the molar volume which confirms that the doping of Er^{+3} beyond 1 mol % causes the formation of non-bridging oxygen NBO

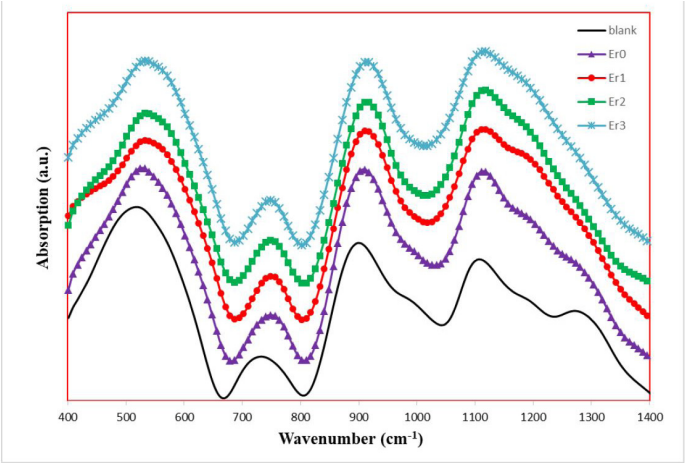

Fig.3: FT-IR absorption spectra of the prepared samples for different concentrations of Er^{+3}.

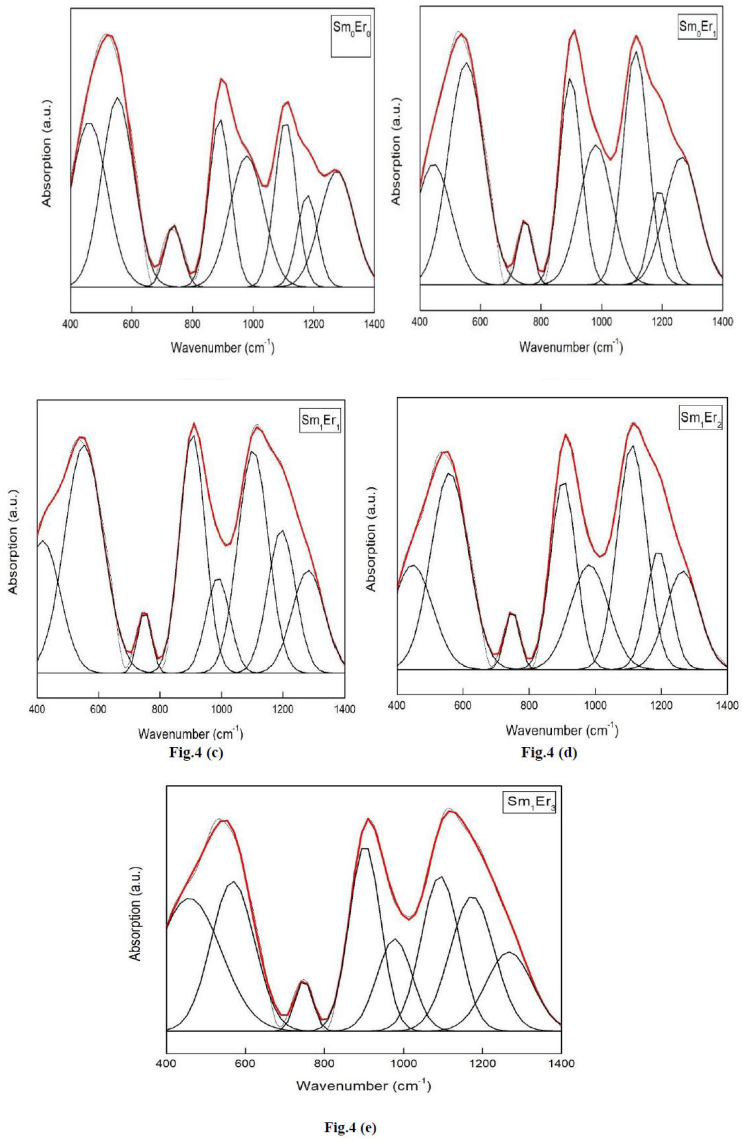

Fig.4: (a,b,c,d,e) FTIR spectra for the presented samples with deconvolution fitting.

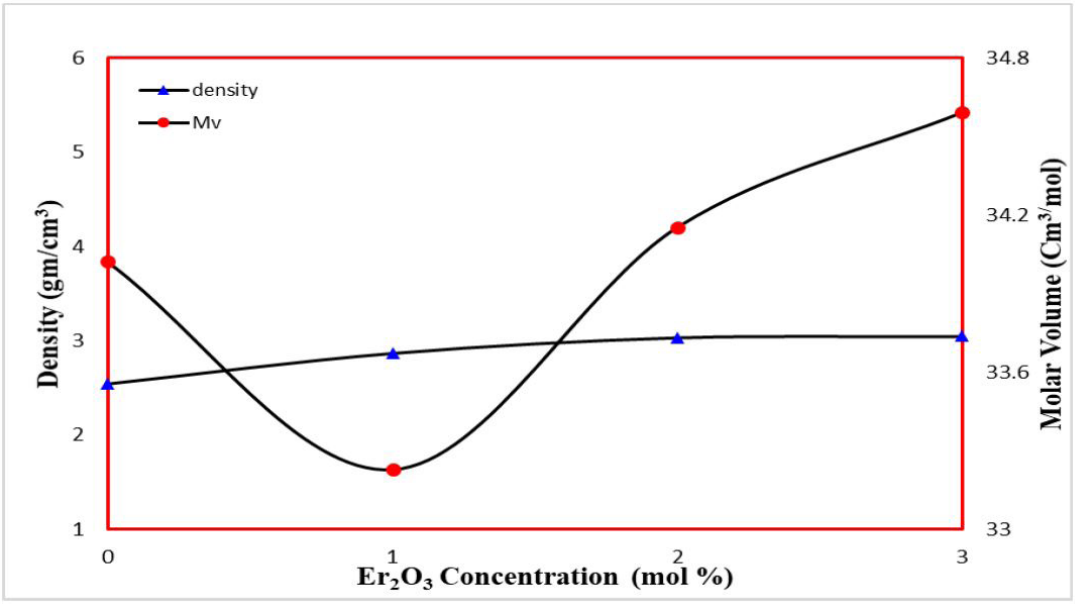

Fig. 5: Density and Molar volume of the prepared samples with different concentrations of Er^{+3} ions.

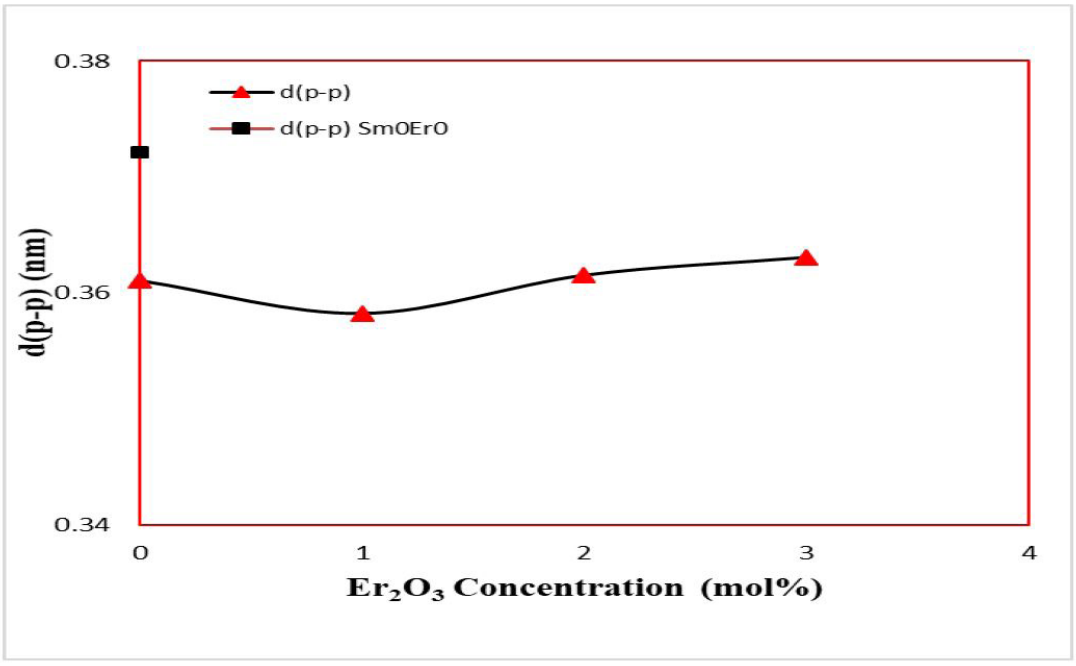

Fig.6: The average distance between phosphorous ions, d_{p-p} with different concentrations of Er^{+3} ions.

TABLE 1: The chemical composition with concentration (mol %) of the prepared samples.

Sample	P_2O_5	ZnO	Li_2O	Na_2O	Sm_2O_3	Er_2O_3
Sm_0Er_0	40	20	10	30	0	0
Sm_0Er_1	40	20	10	29	1	0
Sm_1Er_1	40	20	10	28	1	1
Sm_1Er_2	40	20	10	27	1	2
Sm_1Er_3	40	20	10	26	1	3

TABLE 2: Assignment for the deconvoluted peaks with the vibrational modes.

No.	Vibrational modes	Q modes	Range presented
1	Bending vibration of O—P—O, δ (PO2) modes of (PO-2) chain groups.		447-422
2	Bending vibration of O-P=O		533-551
3	υ_s(P–O–P)	Q2	737-746
4	υ_{as}(P–O–P)	Q2	889-903
5	υ_s(P-O^-)	Q1	969-986
6	υ_{as}(P-O^-)	Q2	1102-1114
7	$\upsilon_s(PO_2)$		1173-1197
8	$\upsilon_{as}(PO_2)$ and Stretching mode of P=O.	Q2	1252-1277

TABLE 3: Ion concentration, the interatomic distance, polaron radius, and field strength with respect to the concentration of Er^{+3} ions.

Sample	Sm_2O_3	Er_2O_3	$N_i \times 10^{20}$ (ion /cm^3)	d_{p-p} (nm)	V_m^p (nm)	F $x10^{14}$ $(cm)^2$
Sm_0Er_0	0	0	0	0	0	0
Sm_1Er_0	1	0	0	0	0	0
Sm_1Er_1	1	1	1.81	1.7	0.71	0.9
Sm_1Er_2	1	2	3.53	1.4	0.57	1.49
Sm_1Er_3	1	3	5.22	1.2	0.50	1.94

which gives a reason for the opening structure phenomena. As shown in Table 3, the space around Er^{+3} ions represented as r_i decreases by increasing the concentration N_i, both the interatomic distance r_i and polaron radius r_p decrease with the increasing of the Er^{+3} ion concentration. This inverse behavior may be attributed to the increase in the field strength between atoms or the stretching force constant F[38].

Conclusion

Samarium oxide doped phosphate glasses with different concentrations of Er^{+3} ions were prepared using a melt quenching technique. The XRD pattern proved the amorphousity nature of the prepared glasses. SEM analysis enhanced the X-ray results. The data evaluated using EDAX and the elements' concentration existed in the batch are in a reasonable agreement. The quantitative analysis using FTIR demonstrated the transformation from Q^3 sites into Q^2 and Q^1 with no evidence of Q^0 site confirming the presence of NBO. The measured density increased by the influence of the concentration of Er^{+3} ions. The molar volume revealed the formation of NBO. The inversely proportional between interatomic distance, polaron radius, and field strength also confirmed the change in the glass network structure due to the formation of NBO.

Acknowledgment

Thanks for the great scientifical comments of prof. Lotfia El Nadi during Modern trends in physics research conference.

References

1. Rivera-López F, Babu P, Jyothi L, et al. Er3+-Yb3+ codoped phosphate glasses used for an efficient 1.5 μm broadband gain medium. *Opt Mater (Amst)*. 2012;34(8):1235-1240. doi:10.1016/j.optmat.2012.01.017

2. Sójka L, Tang Z, Furniss D, et al. Broadband, mid-infrared emission from Pr3+doped GeAsGaSe chalcogenide fiber, optically clad. *Opt Mater (Amst)*. 2014;36(6):1076-1082. doi:10.1016/j.optmat.2014.01.038

3. Wang HQ, Batentschuk M, Osvet A, Pinna L, Brabec CJ. Rare-earth ion doped up-conversion materials for photovoltaic applications. *Adv Mater*. 2011;23(22-23):2675-2680. doi:10.1002/adma.201100511

4. Chen L, He D, Luan F, Hu L, Chen W. An efficient erbium doped phosphate laser glass for high average power pumping. 2009;482:261-263. doi:10.1016/j.jallcom.2009.03.173

5. Hajer SS, Halimah MK, Azmi Z, Azlan MN. Optical properties of Zinc-Borotellurite doped samarium. *Chalcogenide Lett*. 2014;11(11):553-566. doi:10.1080/02666281003771190

6. Aronne A, Esposito S, Pernice P. FTIR and DTA study of lanthanum aluminosilicate glasses. *Mater Chem Phys*. 1997;51(2):163-168. doi:10.1016/S0254-0584(97)80287-8

7. Pugliese D, Boetti NG, Lousteau J, et al. Concentration quenching in an Er-doped phosphate glass for compact optical lasers and amplifiers. *J Alloys Compd*. 2016;657:678-683. doi:10.1016/j.jallcom.2015.10.126

8. Rasool SN, Jamalaiah BC, Suresh K, Moorthy LR, Jayasankar CK. Spectroscopic properties of Er3+-doped phosphate based glasses for broadband 1.54 μm emission. *J Mol Struct*. 2017;1130:837-843. doi:10.1016/j.molstruc.2016.10.090

9. Liang X, Li H, Wang C, Yu H, Li Z, Yang S. Physical and structural properties of calcium iron phosphate glass doped with rare earth. *J Non Cryst Solids*. 2014;402(June):135-140. doi:10.1016/j.jnoncrysol.2014.05.021

10. Lofaj F, Satet R, Hoffmann MJ, de Arellano López AR. Thermal expansion and glass transition temperature of the rare-earth doped oxynitride glasses. *J Eur Ceram Soc*. 2004;24(12):3377-3385. doi:10.1016/j.jeurceramsoc.2003.10.012

11. Stoch P, Stoch A, Ciecinska M, Krakowiak I, Sitarz M. Structure of phosphate and iron-phosphate glasses by DFT calculations and FTIR/Raman spectroscopy. *J Non Cryst Solids*. 2016;450:48-60. doi:10.1016/j.jnoncrysol.2016.07.027

12. Sołtys M, Pisarska J, Leśniak M, Sitarz M, Pisarski WA. Structural and spectroscopic properties of lead phosphate glasses doubly doped with Tb3+ and Eu3+ ions. *J Mol Struct*. 2018;1163:418-427. doi:10.1016/j.molstruc.2018.03.021

13. Moustafa YM, El-Egili K. Infrared spectra of sodium phosphate glasses. *J Non Cryst Solids*. 1998;240(1-3):144-153. doi:10.1016/S0022-3093(98)00711-X

14. Lai YM, Liang XF, Yang SY, Wang JX, Cao LH, Dai B. Raman and FTIR spectra of iron

phosphate glasses containing cerium. *J Mol Struct*. 2011;992(1-3):84-88. doi:10.1016/j.molstruc.2011.02.049

15. Soo S. Structural , thermal and spectroscopic properties of highly Er3 + -doped novel oxyfluoride glasses for photonic application. *Mater Res Bull*. 2014;51:336-344. doi:10.1016/j.materresbull.2013.12.023

16. Gaafar MS, Marzouk SY. Judd–Ofelt analysis of spectroscopic properties of Er3+doped TeO2-BaO-ZnO glasses. *J Alloys Compd*. 2017;723:1070-1078. doi:10.1016/j.jallcom.2017.06.261

17. Hraiech S, Ferid M, Guyot Y, Boulon G. Structural and optical studies of Yb3+, Er3+and Er3+/Yb3+co-doped phosphate glasses. *J Rare Earths*. 2013;31(7):685-693. doi:10.1016/S1002-0721(12)60343-3

18. Li GS, Zhang CM, Zhu PF, Jiang C, Song P, Zhu K. Broadband near-infrared emission in Pr3+-Er3+codoped phosphate glasses for optical amplifiers. *Ceram Int*. 2016;42(4):5558-5561. doi:10.1016/j.ceramint.2015.12.026

19. Bahadur A, Dwivedi Y, Rai SB. Spectroscopic study of Er:Sm doped barium fluorotellurite glass. *Spectrochim Acta - Part A Mol Biomol Spectrosc*. 2010;77(1):101-106. doi:10.1016/j.saa.2010.04.033

20. Borate I, Containing G, Ions T. Infrared Absorption Spectra of Some Gamma Irradiated Borate Glasses Containing Nickel and Titanium Ions. 2011;637(6).

21. Glasses B, Antibacterial C. Processing, Characterization and Application of Some Borophosphate Glasses Containing Antibacterial and Antifungal Oxides in Bioactive Demands. 2018;173(1):163-173. doi:10.21608/EJCHEM.2018.2229.1184

22. El Mesady I, Alawsh S. Optical and luminescence properties of silicon doped alumino-phosphate-sodium glass system. *J Non Cryst Solids*. 2018;482(October 2017):236-242. doi:10.1016/j.jnoncrysol.2017.12.054

23. Moustafa MG, Morshidy H, Mohamed AR, El-Okr MM. A comprehensive identification of optical transitions of cobalt ions in lithium borosilicate glasses. *J Non Cryst Solids*. 2019;517(February):9-16. doi:10.1016/j.jnoncrysol.2019.04.037

24. B Edathazhe A, Shashikala HD. Effect of BaO addition on the structural and mechanical properties of soda lime phosphate glasses. *Mater Chem Phys*. 2016;184:146-154. doi:10.1016/j.matchemphys.2016.09.035

25. Abdelghany AM, Elbatal FH, Elbatal HA, EzzElDin FM. Optical and FTIR structural studies of CoO-doped sodium borate, sodium silicate and sodium phosphate glasses and effects of gamma irradiation - A comparative study. *J Mol Struct*. 2014;1074:503-510. doi:10.1016/j.molstruc.2014.06.011

26. Langar A, Bouzidi C, Elhouichet H, Gelloz B, Ferid M. Investigation of spectroscopic properties of Sm-Eu codoped phosphate glasses. *Displays*. 2017;48:61-67. doi:10.1016/j.displa.2017.03.004

27. Jlassi I, Sdiri N, Elhouichet H. Electrical conductivity and dielectric properties of MgO doped lithium phosphate glasses. *J Non Cryst Solids*. 2017;466-467:45-51. doi:10.1016/j.jnoncrysol.2017.03.042

28. Pisarski WA, Zur L, Goryczka T, Sołtys M, Pisarska J. Structure and spectroscopy of rare earth - Doped lead phosphate glasses. *J Alloys Compd*. 2014;587:90-98. doi:10.1016/j.jallcom.2013.10.106

29. Lu M, Wang F, Chen K, Dai Y, Liao Q, Zhu H. The crystallization and structure features of barium-iron phosphate glasses. *Spectrochim Acta - Part A Mol Biomol Spectrosc*. 2015;148:1-6. doi:10.1016/j.saa.2015.03.121

30. Rani S, Sanghi S, Agarwal A, Seth VP. Study of optical band gap and FTIR spectroscopy of Li2O·Bi2O3·P2O5 glasses. *Spectrochim Acta - Part A Mol Biomol Spectrosc*. 2009;74(3):673-677. doi:10.1016/j.saa.2009.07.023

31. Electrical and Structural Properties of Nickel Oxide - Containing Phosphate Glasses. 2010;99(1):85-99.

32. Afef B, Hegazy HH, Algarni H, et al. Spectroscopic analysis of trivalent Nd3+/Yb3+ions codoped in PZS host glasses as a new laser material at 1.06 μm. *J Rare Earths*. 2017;35(4):361-367. doi:10.1016/S1002-0721(17)60920-7

33. Upender G, Ramesh S, Prasad M, Sathe VG, Mouli VC. Optical band gap, glass transition temperature and structural studies of (100 - 2x) TeO2-xAg2O-xWO3glass system. *J Alloys*

Compd. 2010;504(2):468-474. doi:10.1016/j.jallcom.2010.06.006

34. Saddeek YB, Shaaban ER, Moustafa ES, Moustafa HM. Spectroscopic properties, electronic polarizability, and optical basicity of Bi2O3-Li2O-B2O3 glasses. *Phys B Condens Matter*. 2008;403(13-16):2399-2407. doi:10.1016/j.physb.2007.12.027

35. Kaur S, Singh GP, Kaur P, Singh DP. Cerium luminescence in borate glass and effect of aluminium on blue green emission of cerium ions. *J Lumin*. 2013;143:31-37. doi:10.1016/j.jlumin.2013.04.027

36. Ramesh P, Jagannath G, Eraiah B, Kokila MK. Optical and Physical Investigations of Lanthanum Bismuth Borate glasses doped with Ho2O3. *IOP Conf Ser Mater Sci Eng*. 2018;310(1). doi:10.1088/1757-899X/310/1/012032

37. Elgazery M, Ali AA. Egyptian Journal of Chemistry. 2019;62(4):655-664. doi:10.21608/EJCHEM.2018.5386.1474

38. Jlassi I, Elhouichet H, Ferid M. Influence of MgO on structure and optical properties of alumino-lithium-phosphate glasses. *Phys E Low-Dimensional Syst Nanostructures*. 2016;81:219-225. doi:10.1016/j.physe.2016.03.017